



Tendencias y proyecciones futuras de tormentas y vientos extremos

Prof. Jose Manuel Gutiérrez

Instituto de Física de Cantabria
(CSIC - Universidad de Cantabria)
gutierjm@unican.es



SEMINARIOS DEL PLAN NACIONAL DE ADAPTACIÓN AL
CAMBIO CLIMÁTICO



IMPACTOS Y ADAPTACIÓN AL
CAMBIO CLIMÁTICO EN EL SECTOR DEL
SEGURIDAD

27 y 28 de noviembre de 2017

Centro Nacional de Educación Ambiental
(CENEAM)
Valsain, Segovia.

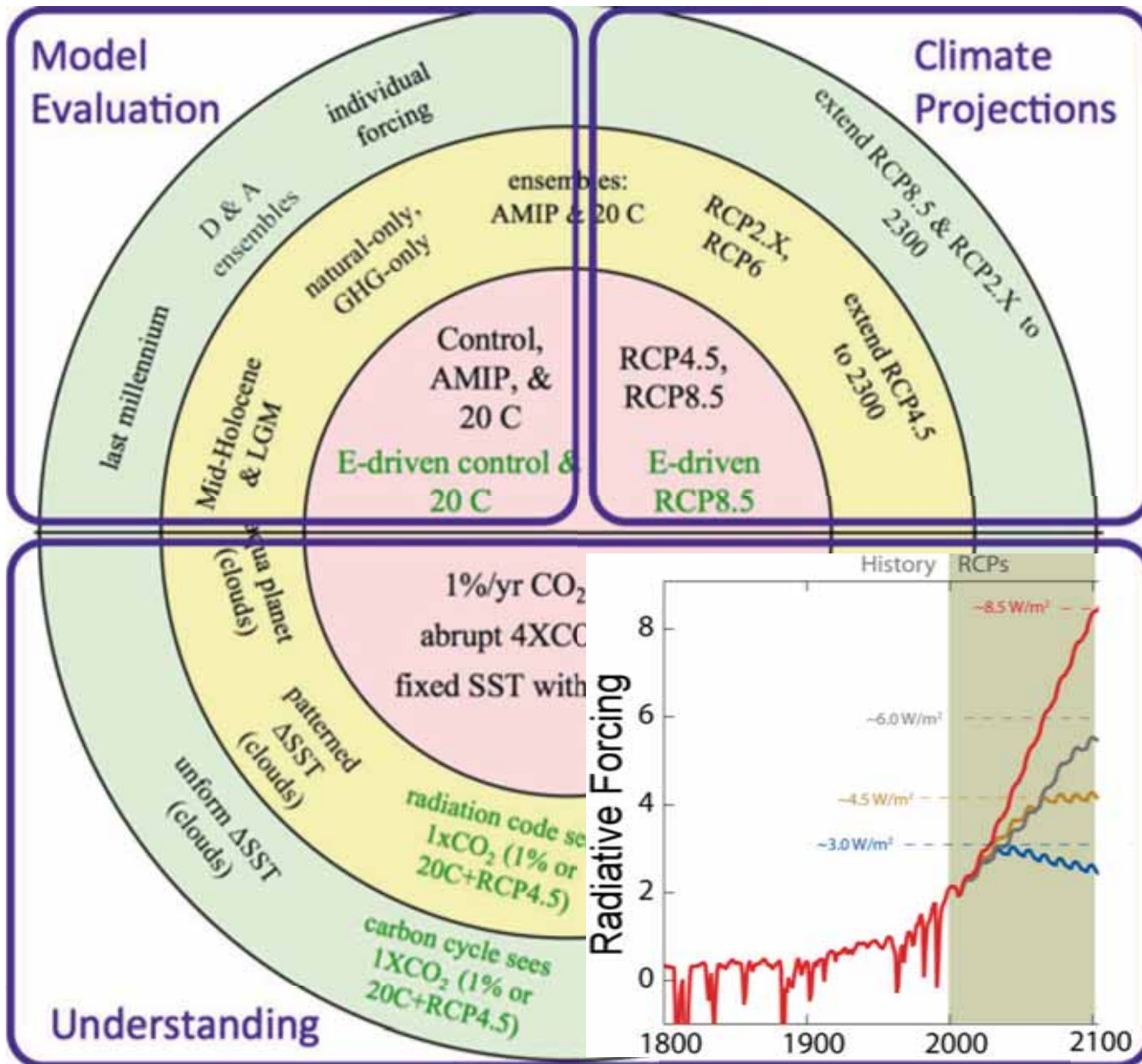
Contacto: cblasco@mapama.es
www.lifeshara.com

Proyecciones Regionales de
Cambio Climático Para Vientos
Extremos en España Para el
Siglo XXI

Julio 2017 - Junio 2018



MINISTERIO
DE AGRICULTURA, ALIMENTACIÓN
Y MEDIO AMBIENTE

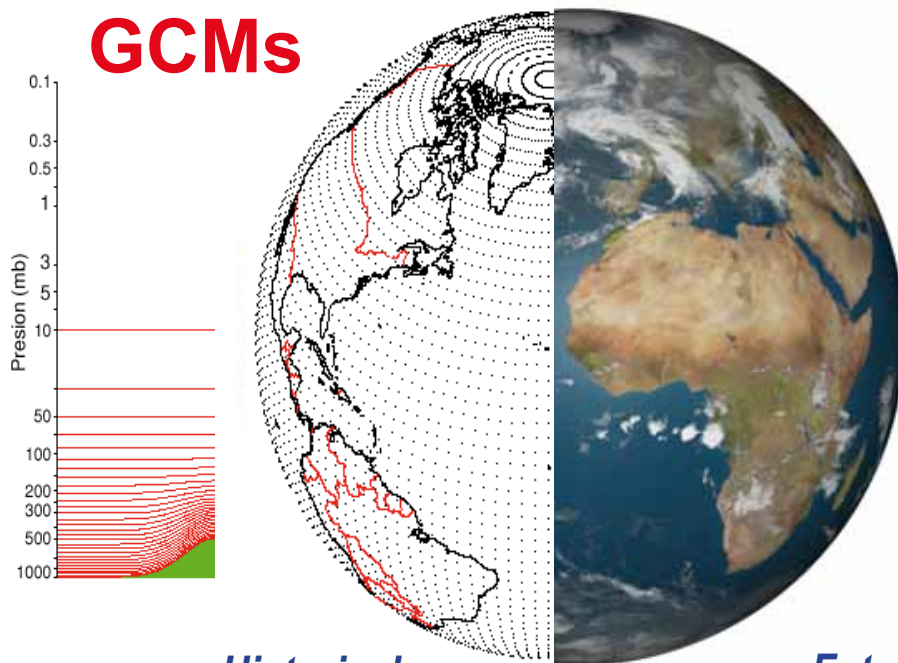


Multi-decadal forcing conditions are given for a number of historical and future scenarios for model validation and climate change attribution and projection.



Climate change projections

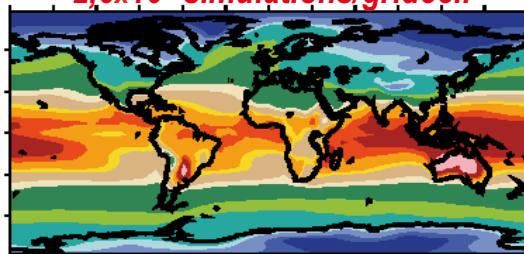
GCMs



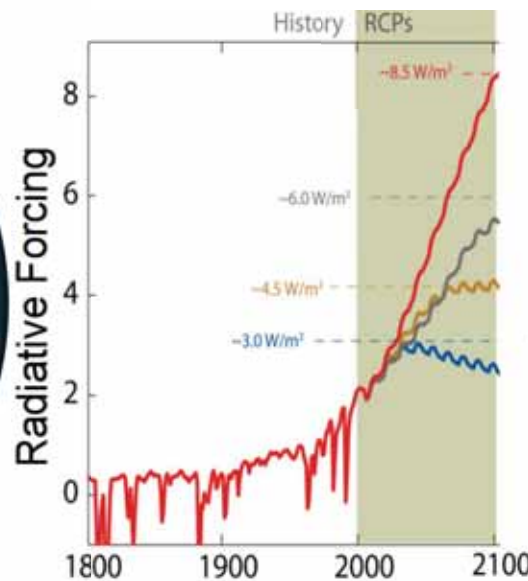
Historical simulations

1980 1990 2000

1h step x 30 years
 2.6×10^5 simulations/gridcell

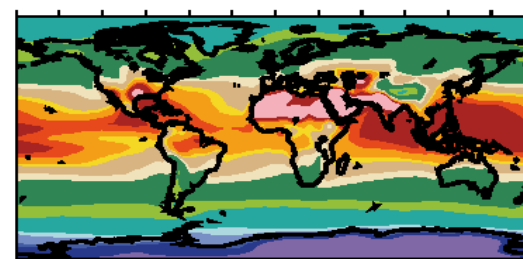


235 245 255 265 275 285 295 297 299 301
230 240 250 260 270 280 290 292.5 296 298 300 302



Future projections
(scenarios)

2010 2020 2030 2040 2050 2060 2070 2080 2090

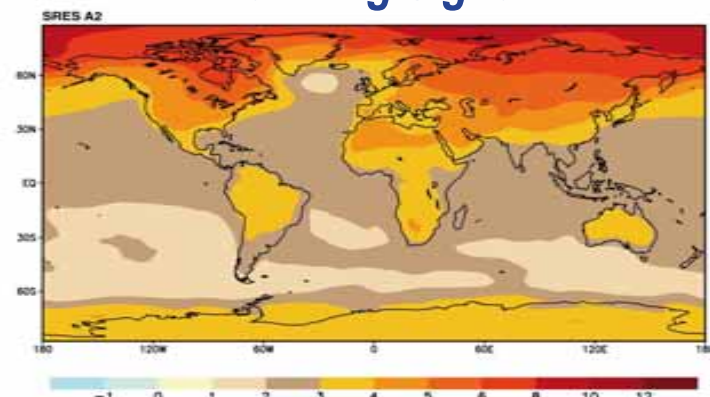


Equations of conservation
(mass,momentum,energy,water vapour)
and gas state

$$\mathbf{v} = (u, v, w), T, p, \rho = 1/\alpha \text{ and } q$$

$$\left\{ \begin{array}{lcl} \frac{d\mathbf{v}}{dt} & = & -\alpha \nabla p - \nabla \phi + \mathbf{F} - 2\Omega \times \mathbf{v} \\ \frac{\partial \rho}{\partial t} & = & -\nabla \cdot (\rho \mathbf{v}) \\ p \alpha & = & RT \\ Q & = & C_p \frac{dT}{dt} - \alpha \frac{dp}{dt} \\ \frac{\partial \rho q}{\partial t} & = & -\nabla \cdot (\rho \mathbf{v} q) + \rho (E - C) \end{array} \right.$$

“delta” method
Warming signal



Computational (and physical) constraints limit the resolution (~100-200 Km)

Santander Meteorology Group

A multidisciplinary approach for weather & climate

Multi-Model climate projections

| Climate Models | B |
|------------------|--|
| BCC-CSM1-1 | 0.97 |
| CanESM2_esm | 0.76 |
| CanESM2 | 0.77 |
| CCSM4 | 1.08 |
| CESM1-BGC_esm | 1.06 |
| CESM1-CAM5 | 0.94 |
| CESM1-WACCM | 1.04 |
| CNRM-CM5 | 0.90 |
| CSIRO-ACCESS1-0 | 0.91 |
| CSIRO-Mk3-6-0 | 0.93 |
| FGOALS-g2 | 1.10 |
| FGOALS-s2 | 0.83 |
| GFDL-CM3 | 0.92 |
| GFDL-ESM2G_esm | 1.04 |
| GFDL-ESM2M_esm | 1.05 |
| GFDL-ESM2M | 1.06 |
| GISS-E2-H | 0.96 |
| GISS-E2-R | 0.96 |
| HadGEM2-CC | 0.88 |
| HadGEM2-ES_esm | 0.91 |
| HadGEM2-ES | 0.90 |
| INMCM4_esm | 0.93 |
| IPSL-CM5A-LR_esm | 0.77 |
| IPSL-CM5A-LR | 0.77 |
| IPSL-CM5A-MR | 0.79 |
| IPSL-CM5B-LR | 0.83 |
| MIROC5 | 0.99 |
| MIROC-ESM_esm | 1.14 |
| MIROC-ESM | 1.17 |
| MPI-ESM-LR_esm | 1.15 |
| MPI-ESM-P | 0.88 |
| MRI-CGCM3 | 0.88 |
| MRI-ESM1_esm | 0.84 |
| NorESM1-M | 0.85 |
| Ensemble Mean | $B = \frac{\sum_{i=1}^n P_{\text{CMIPS}}}{\sum_{i=1}^n P_{\text{GPCP}}}$ |
| Ensemble Median | 0.85 |



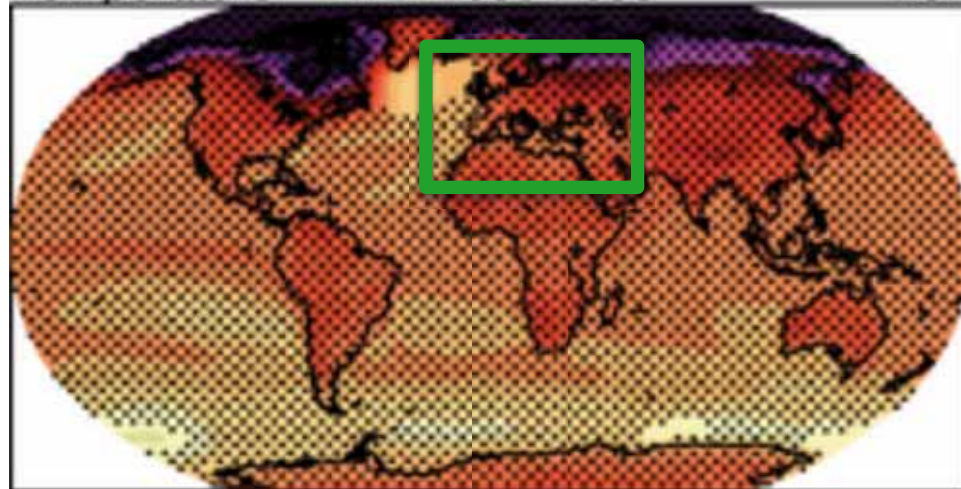
Climate change projections are based on consensus multi-model information.

^aOptimal values of these metrics are all equal to 1.

Multi-Model climate projections

Santander Meteorology Group
A multidisciplinary approach for weather & climate

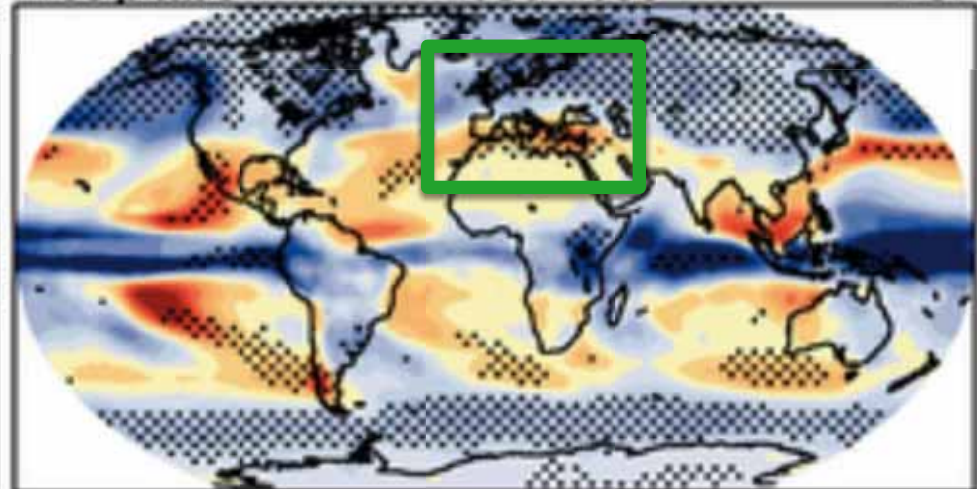
Temperature A1B: 2080-2099



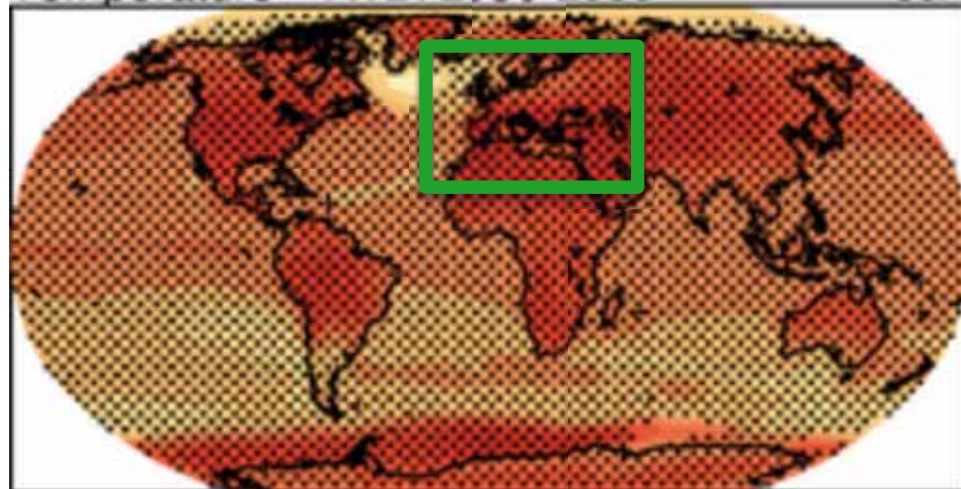
DJF Precipitation

A1B: 2080-2099

DJF



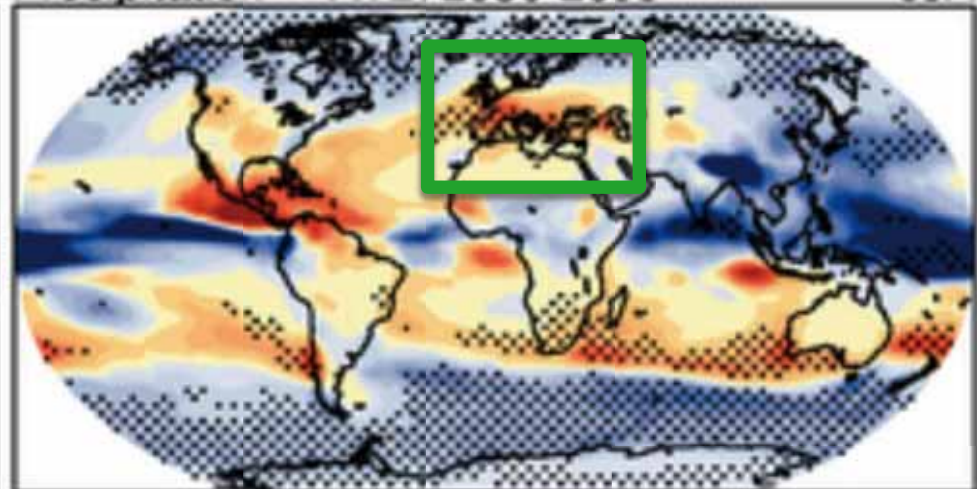
Temperature A1B: 2080-2099



JJA Precipitation

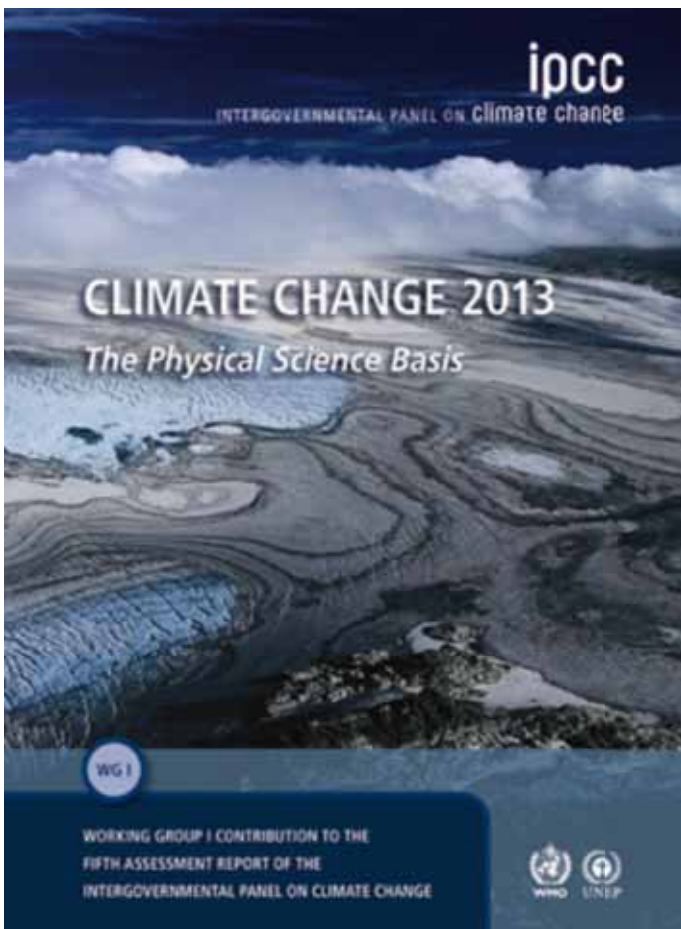
A1B: 2080-2099

JJA



The different IPCC Assessment Reports provide no information on future wind projections, only inconclusive information on past trends.

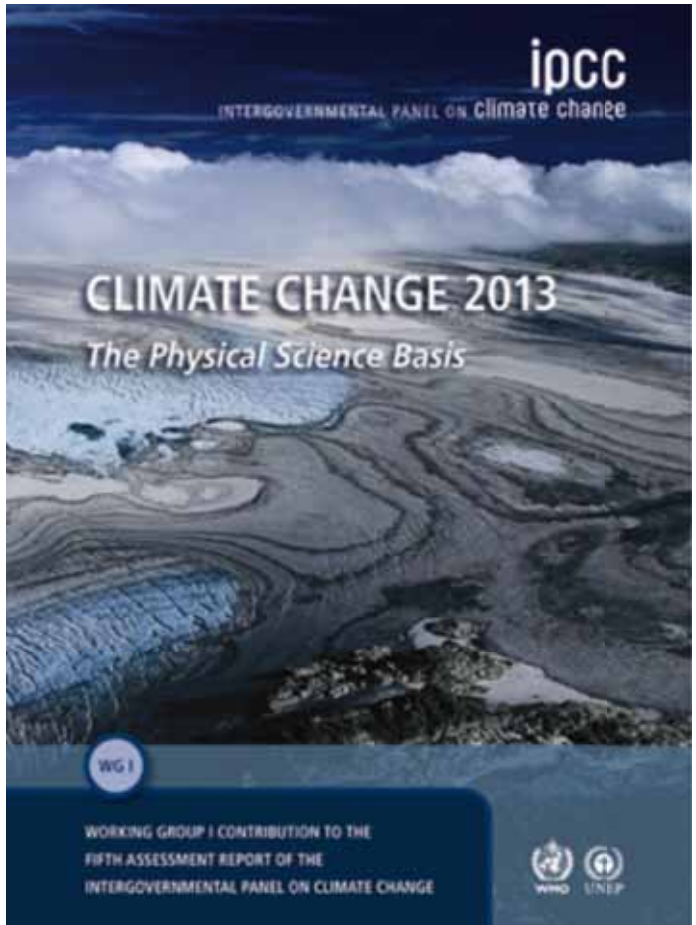
IPCC-AR5 CMIP5 (2013)



Wind in IPCC Reports

The different IPCC Assessment Reports provide no information on future wind projections, only inconclusive information on past trends.

IPCC-AR5 CMIP5 (2013) SRES Special Rep. (2012)



The IPCC special report on climate extremes discussed the existing information on mean and extreme wind projections, obtaining also inconclusive results.

Changes in Climate Extremes and their Impacts on the Natural Physical Environment

Coordinating Lead Authors:
Sonia I. Seneviratne (Switzerland), Neville Nicholls (Australia)

Lead Authors:
David Easterling (USA), Clare M. Goodess (United Kingdom), Shinjiro Kanae (Japan), James Kossin (USA), Yali Luo (China), Jose Marengo (Brazil), Kathleen McInnes (Australia), Mohammad Rahimi (Iran), Markus Reichstein (Germany), Asgeir Sorteberg (Norway), Carolina Vera (Argentina), Xuebin Zhang (Canada)

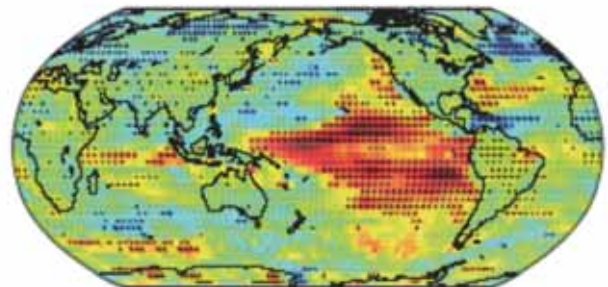
Review Editors:
Matilde Rusticucci (Argentina), Vladimir Semenov (Russia)

Santander Meteorology Group

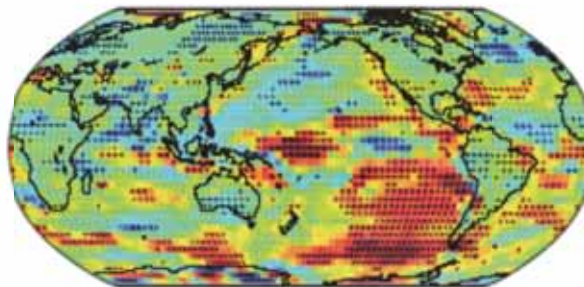
A multidisciplinary approach for weather & climate

Past trends

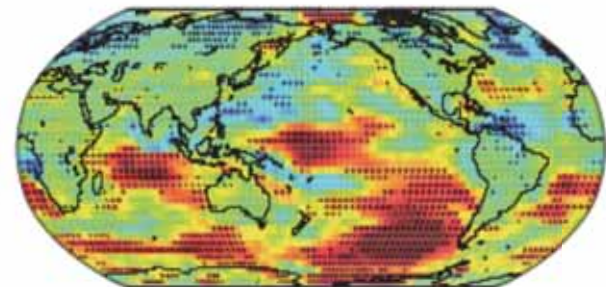
(d) ERA-Interim



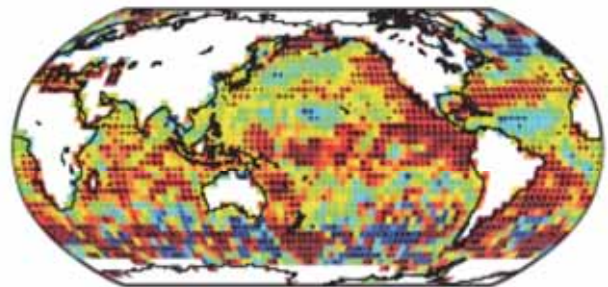
(e) NNR



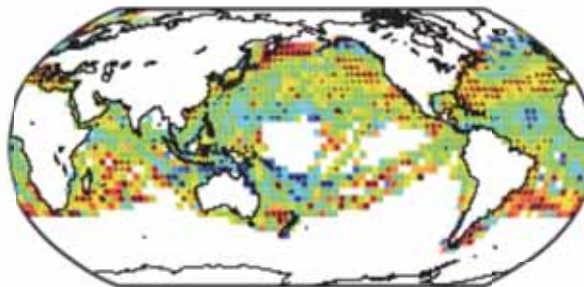
(f) 20CR



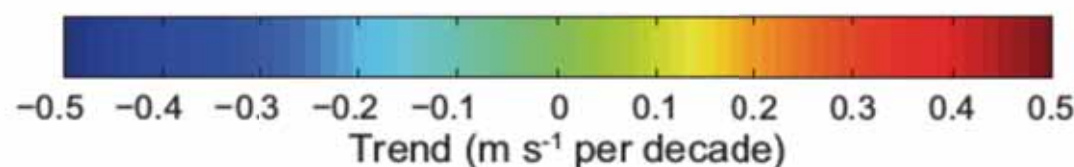
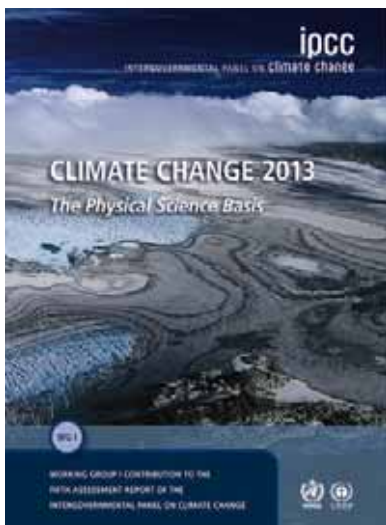
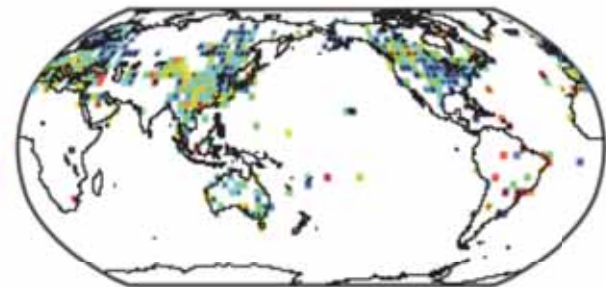
(g) NOCS v2.0



(h) WASWind

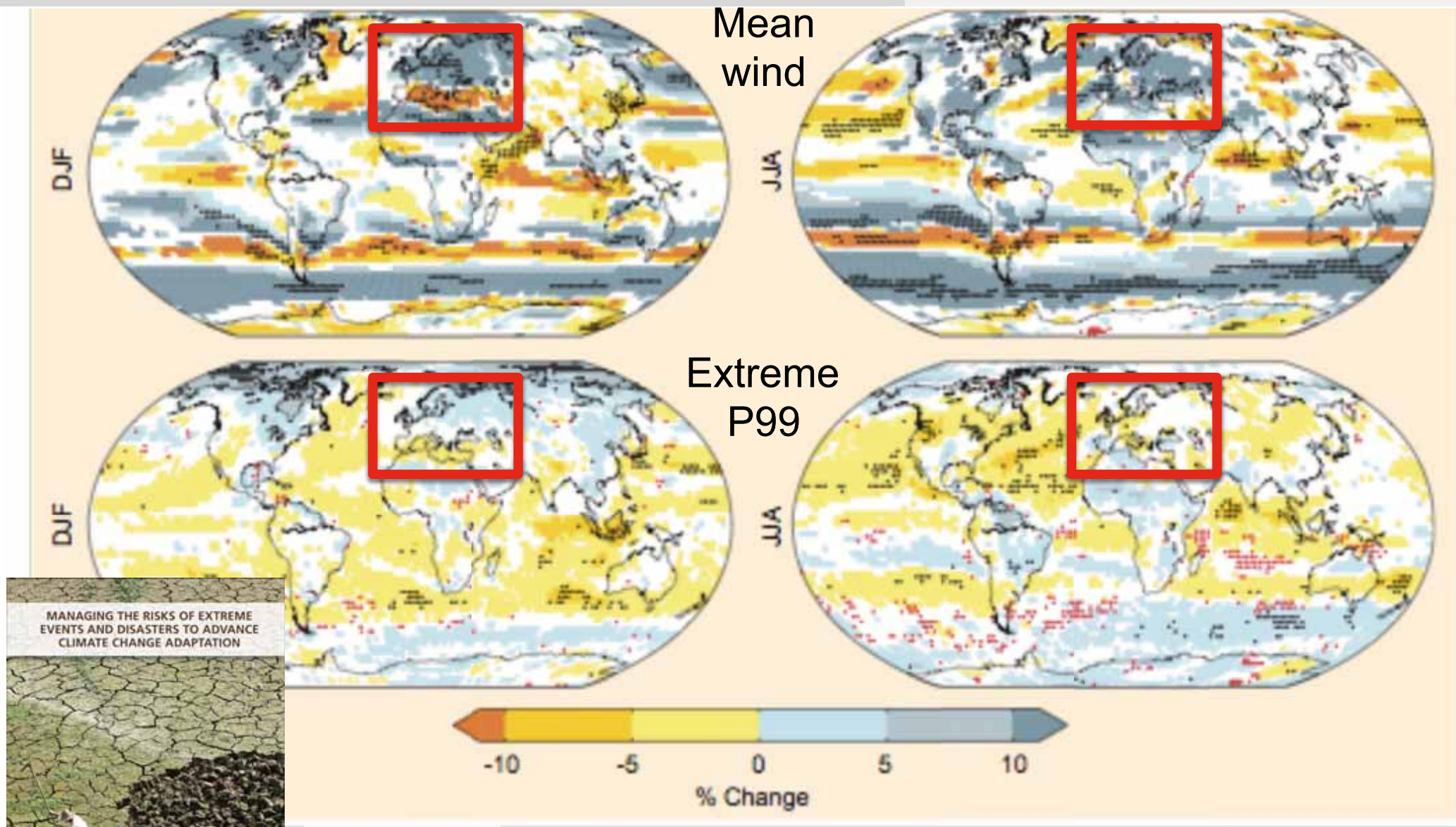


(i) Surface winds on the land

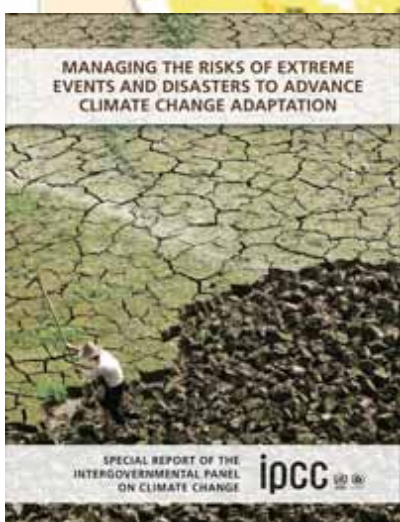


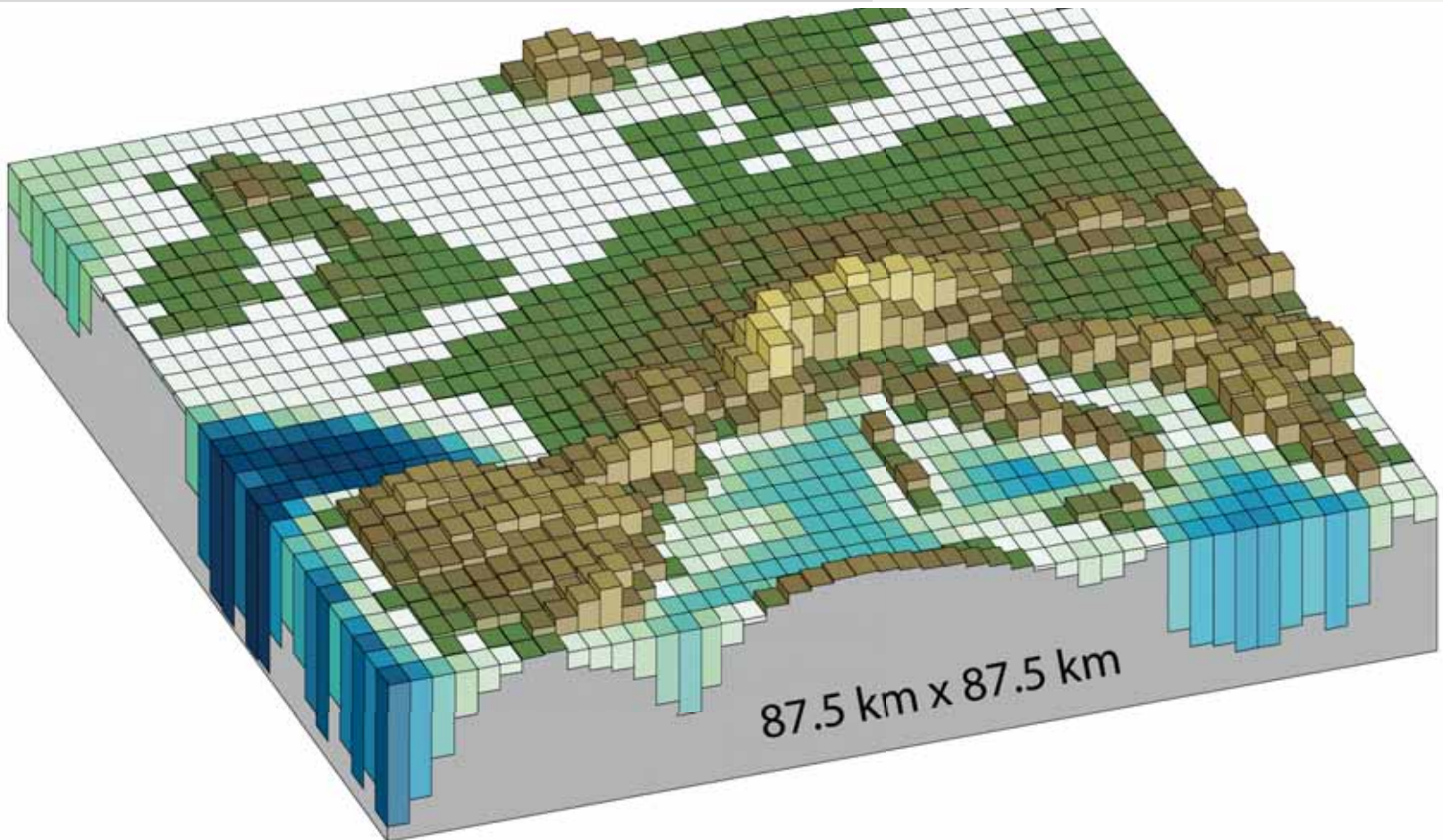
In summary, *confidence is low* in changes in surface wind speed over the land and over the oceans owing to remaining uncertainties in data sets and measures used.

Future projections



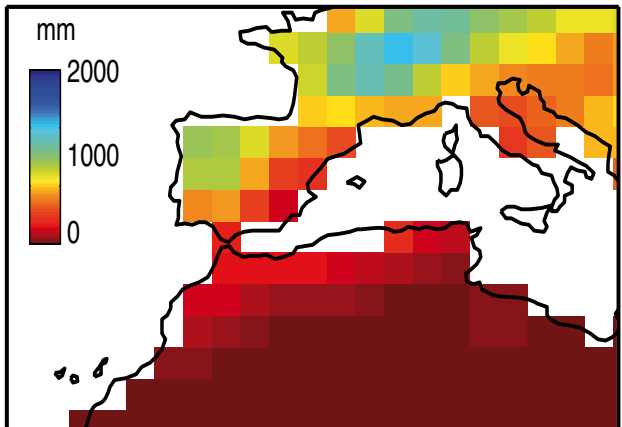
mean that we have **low confidence** in projections of changes in
extreme winds (with the exception of changes associated with





The coarse resolution used to solve GCMs and the empirical representation of sub-grid processes (model parameterizations) severely **limit** the suitability of the GCMs to represent regional/local climate variability, particularly for surface variables (e.g. wind).

MODEL SPACE



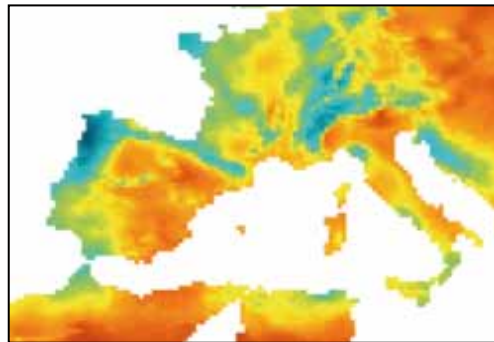
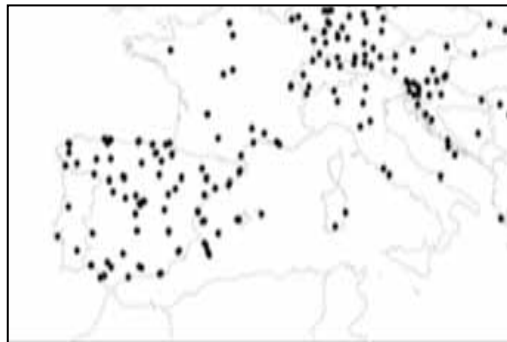
GCM outputs (~200 km)

| Variables | Description | Units |
|------------------|-------------------------------|------------------|
| <i>tas</i> | 2-meter temperature | K |
| <i>tasmax</i> | Daily maximum 2-m temperature | K |
| <i>tasmin</i> | Daily minimum 2-m temperature | K |
| <i>wss</i> | 10 m wind speed | m/s |
| <i>wssmax</i> | Daily maximum 10 m wind speed | m/s |
| <i>hurs</i> | 2-meter relative humidity | % |
| <i>tdps</i> | 2-meter dew point temperature | K |
| <i>psl</i> | Mean sea level pressure | Pa |
| <i>pr</i> | Precipitation | Mm |
| <i>evpsbl</i> | Evaporation | Mm |
| <i>evpsblpot</i> | Potential Evapotranspiration | Mm |
| <i>rss</i> | Net SW surface radiation | W/m ² |
| <i>rls</i> | Net LW surface radiation | W/m ² |
| <i>rsds</i> | Downward SW surface radiation | W/m ² |
| <i>rlds</i> | Downward LW surface radiation | W/m ² |

MODEL BIASES

RESOLUTION

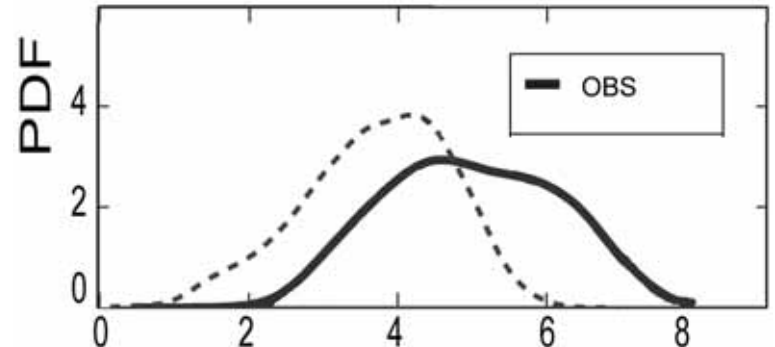
REAL WORLD



Local data (points) Gridded data (~10 km)

[subdaily, daily temporal scale]

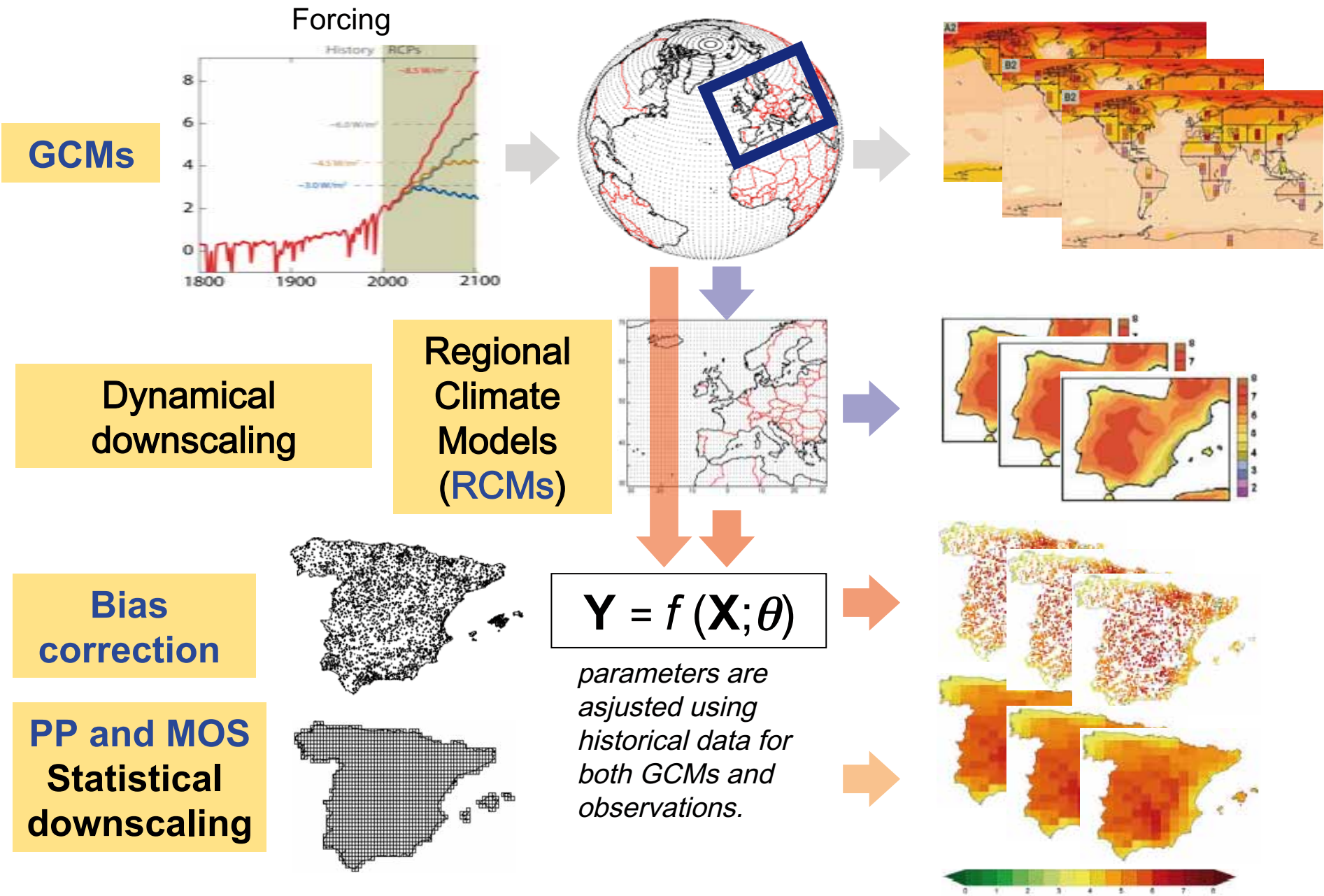
- Hydrology - Energy
- Agriculture - Insurance



Models exhibit biases when compared with observations:

1. Systematic model biases
2. Different resolutions

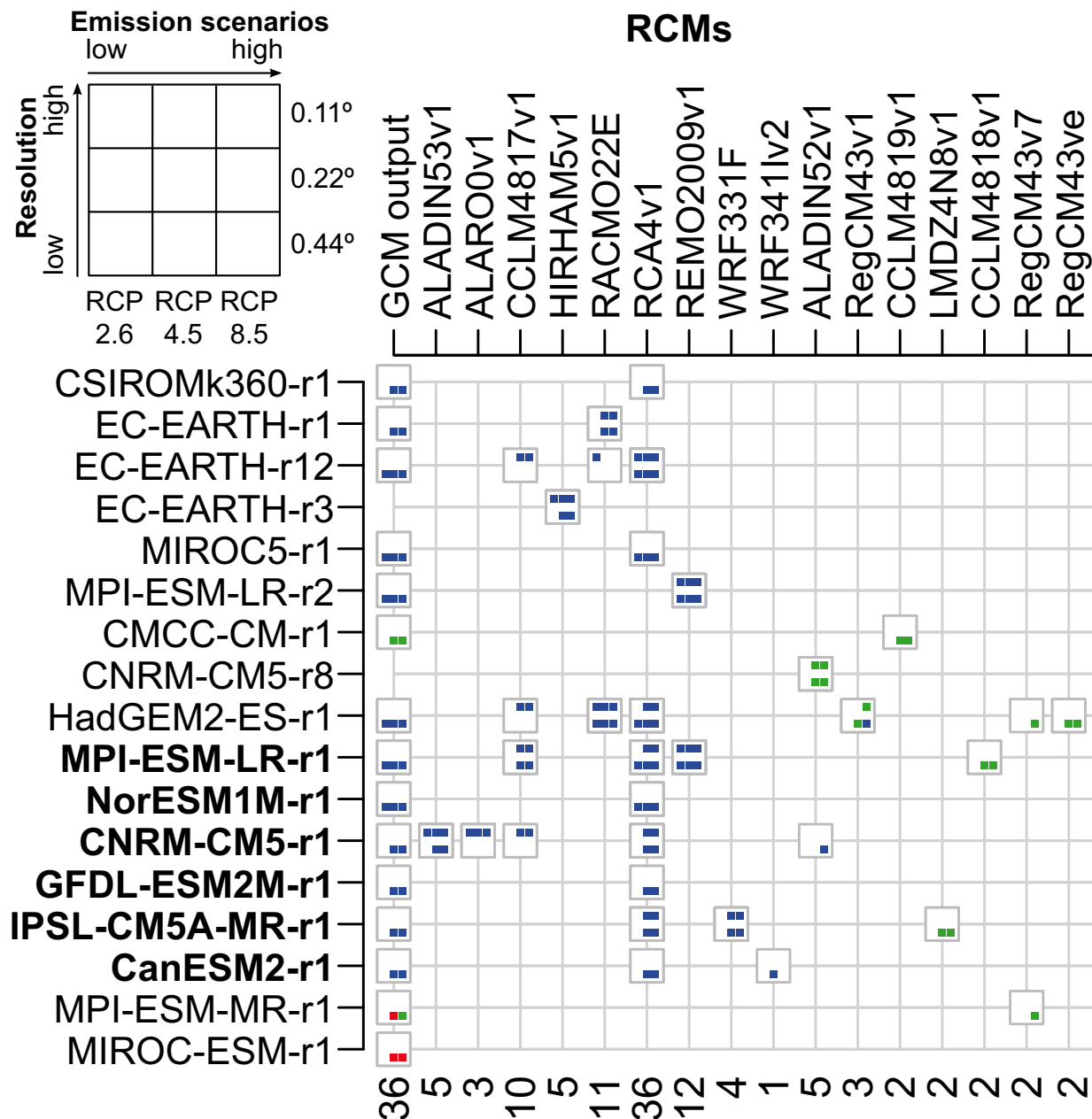
Statistical Downscaling (SDM)





Euro-CORDEX is the last of a series of international initiatives for regional climate change projection over Europe.

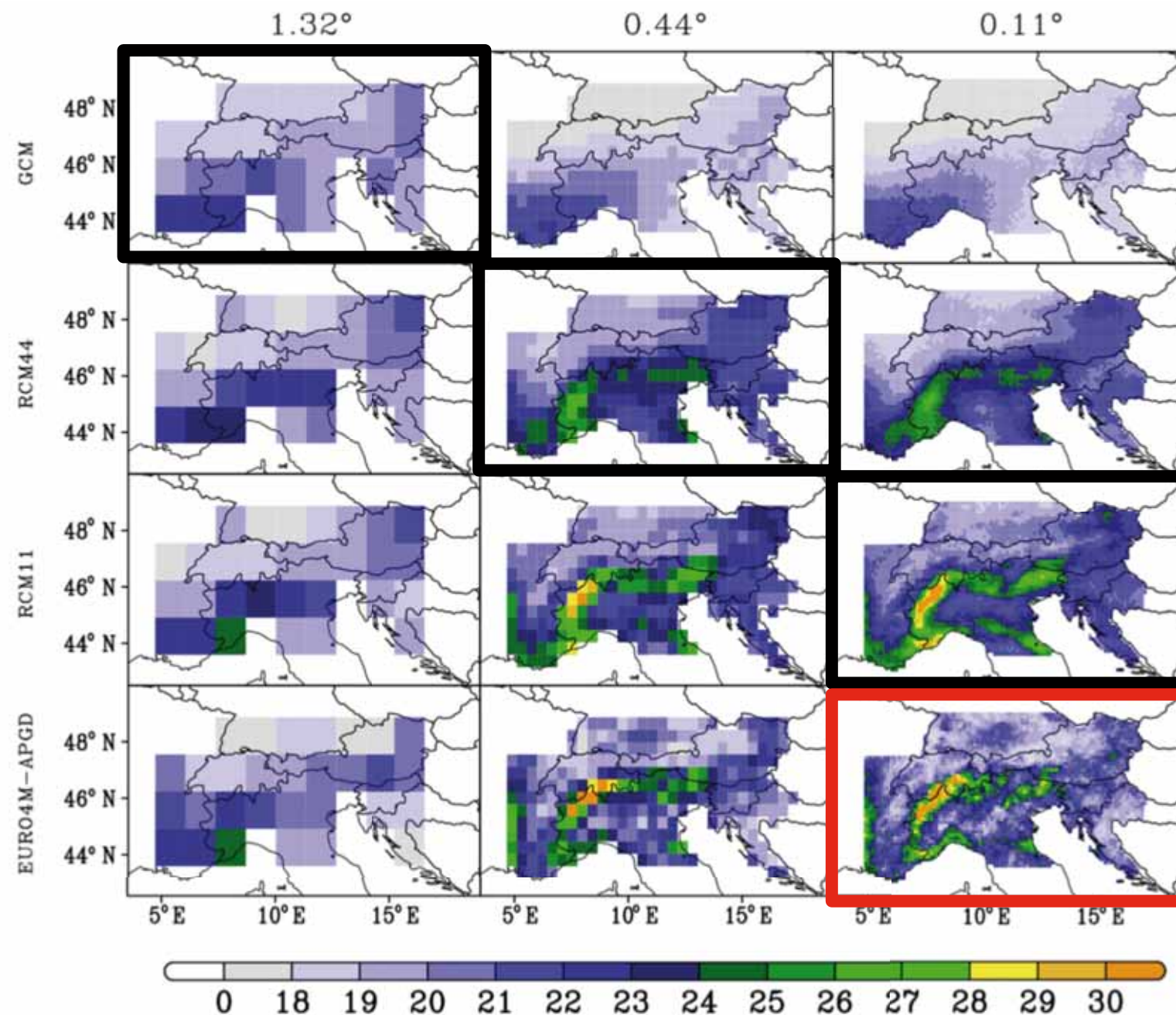
0.11° and **0.44°** resolution.



Santander Meteorology Group

A multidisciplinary approach for weather & climate

EURO-CORDEX



 atmosphere

Review

Review on the Projections of Future Storminess over the North Atlantic European Region

Tina Möller¹, Dirk Schindler^{1,*}, Axel Tim Albrecht² and Ulrich Kohnle²

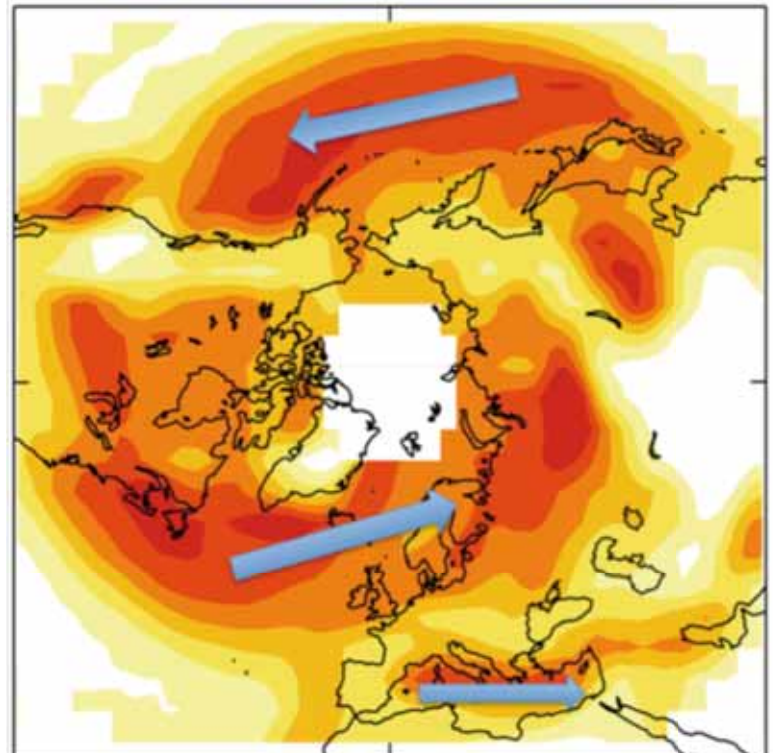
Received: 16 February 2016; Accepted: 15 April 2016; Published: 22 April 2016

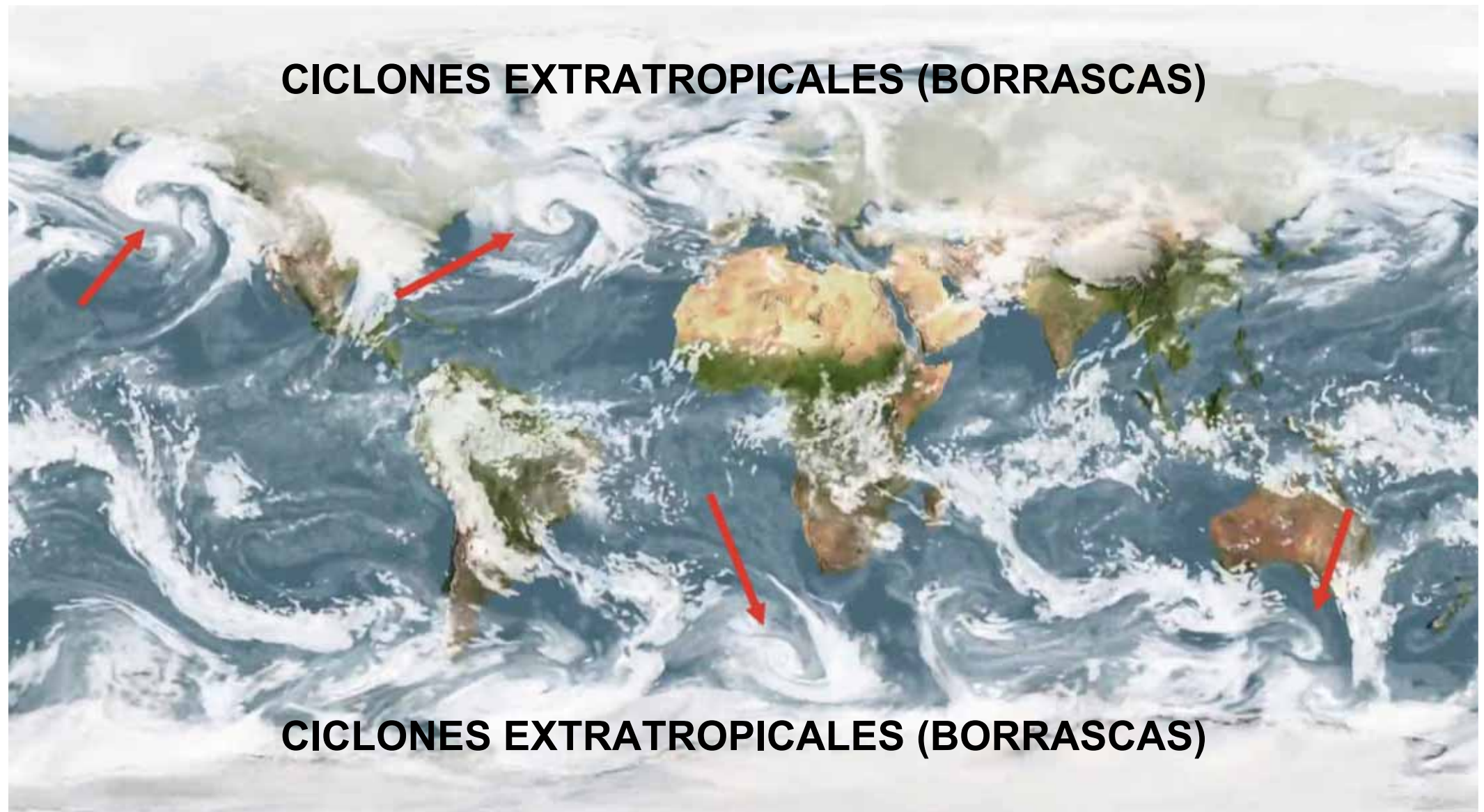


Storm intensity can be characterized by wind speed at 10 m above the ground. In the reviewed literature, it was reported as:

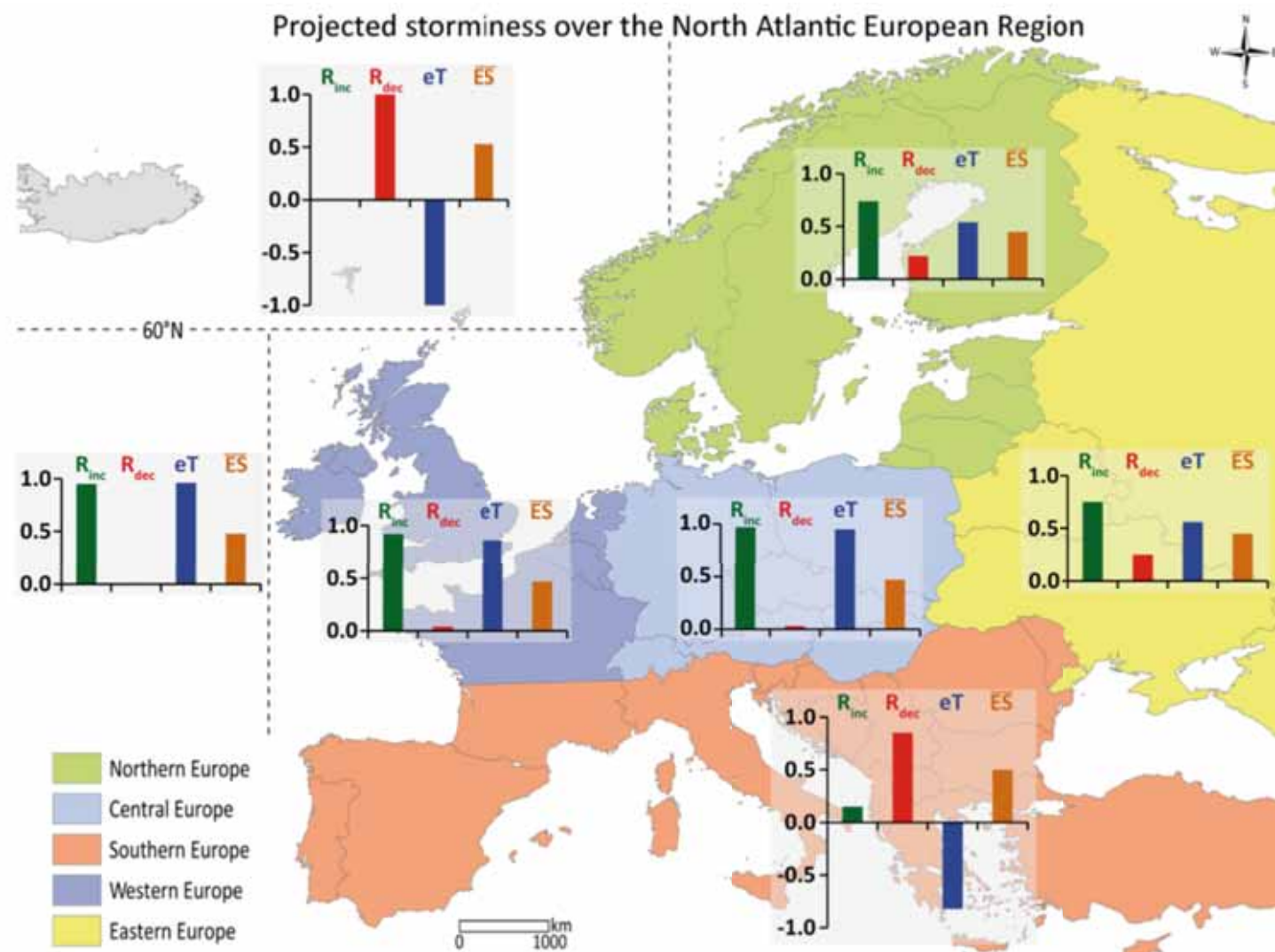
- (i) peak 1-3 s wind gust speed;
- (ii) mean 10 min wind speed; or
- (iii) percentiles (e.g., 90–98 percentiles) of maximum daily wind speed values.

Extratropical cyclones can be defined as a minimum in the mean SLP field or at the 1000 hPa geopotential height → “storm track”





For Southern Europe (Mediterranean) “unambiguously suggests a decreasing tendency of the projected future extratropical storminess”



Most studies focused on Winter !!!

| Study | Model(s) | Category | Reference Period(s), Projection Period(s), Month(s), Season | Region(s) |
|-------------------------------------|-------------------|---|---|---|
| Zappa <i>et al.</i> (2013) [51] | GCM: 19 RCM: - | Cyclone intensity | 1976–2005, 2070–2099, DJF | Mediterranean region |
| Gastineau and Soden (2009) [64] | GCM: 16 RCM: - | Wind intensity | 1995–2000, 2095–2100, - | Southern Europe |
| Donat <i>et al.</i> (2011) [17] | GCM: 7 RCM: 9 | Wind intensity | 1960–2000, 2021–2050, 2071–2100, October–March | Mediterranean region |
| Nikulin <i>et al.</i> (2011) [66] | GCM: 6 RCM: 1 | Wind intensity | 1961–1990, 2071–2100, - | Europe south of 45°N |
| Schwierz <i>et al.</i> (2010) [27] | GCM: 2 RCM: 2 | Wind intensity | 1961–1990, 2071–2100, October–March | Mediterranean region |
| Bengtsson <i>et al.</i> (2006) [9] | GCM: 1 RCM: - | Cyclone intensity | 1961–1990, 2071–2100, DJF | Mediterranean region (30°N–45°N 0°E–40°E) |
| Bengtsson <i>et al.</i> (2009) [31] | GCM: 1 RCM: - | Frequency of extreme cyclones, cyclone intensity | 1959–1990, 2069–2100, DJF | Southern Europe (30°N–47.5°N, 10°W–40°E) |
| Beniston <i>et al.</i> (2007) [70] | GCM: 1 RCM: 7 | Storm intensity | 1961–1990, 2071–2100, DJF | Southern Europe (Alps and south of the Alps) |
| Fink <i>et al.</i> (2009) [38] | GCM: 1 RCM: 2 | Storm frequency | 1970–1999, 2070–2099, winter | Mediterranean region |
| Giorgi <i>et al.</i> (2004) [63] | GCM: 1 RCM: 1 | Storm activity | 1961–1990, 2071–2100, DJF | Southern Europe |
| Muskulus and Jacob (2005) [77] | GCM: 1 RCM: 1 | Frequency of extreme cyclones | 1961–2099, winter | Mediterranean region |

Extreme events: *Explosive cyclogenesis*

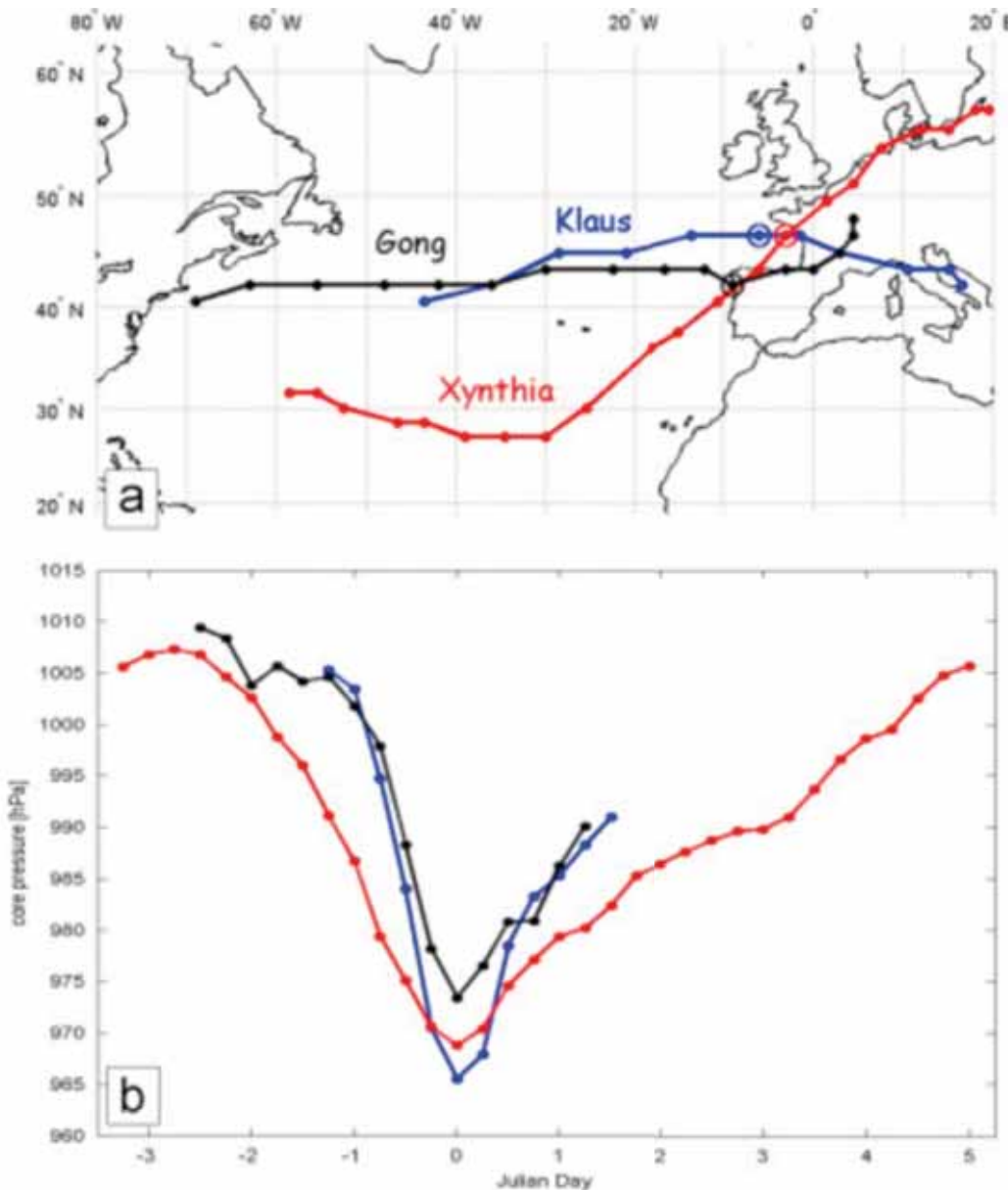


Fig. 2. (a) Cyclone tracks of recent extreme storms over the North Atlantic based on ECMWF ERA-Interim reanalysis data with dots indicating storms' location at six hour intervals: Gong (January 2013, in black), Klaus (January 2009, in blue) and Xynthia (February 2010, in red). The open circle marks the location of the minimum core pressure for each storm. (b) Core pressure evolution over the lifetime of each cyclone (core pressure in hPa). Dates are relative to the minimum core pressure time (zero Julian day).



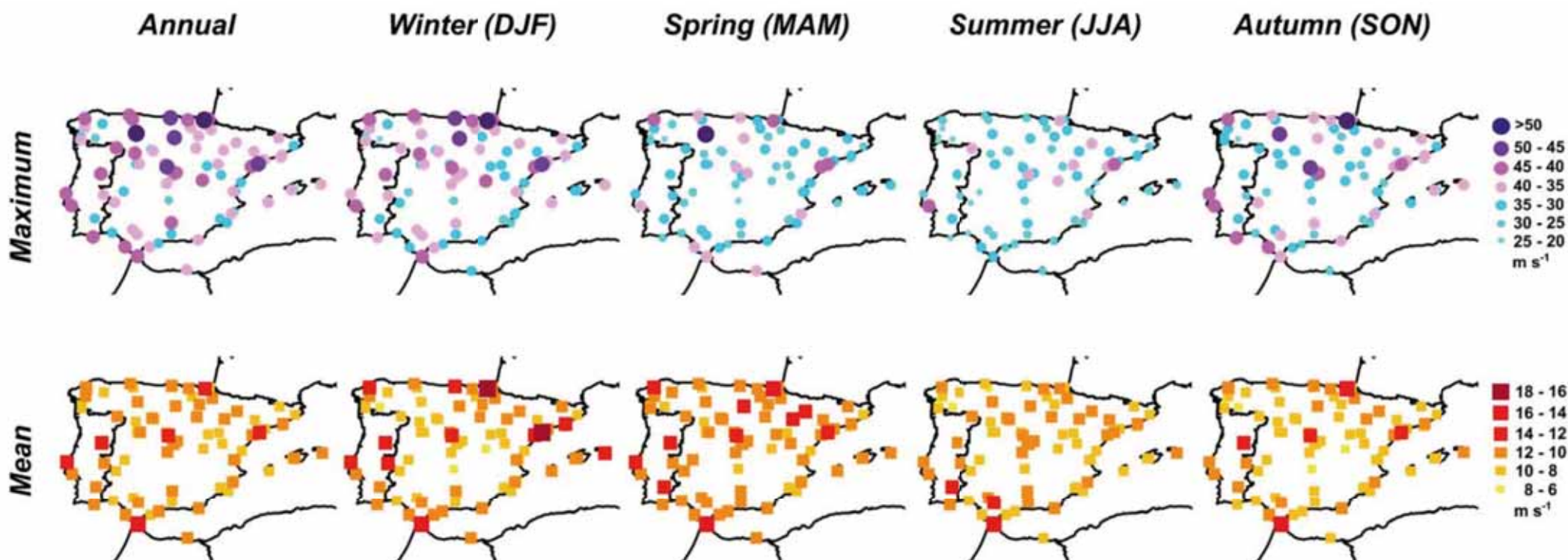
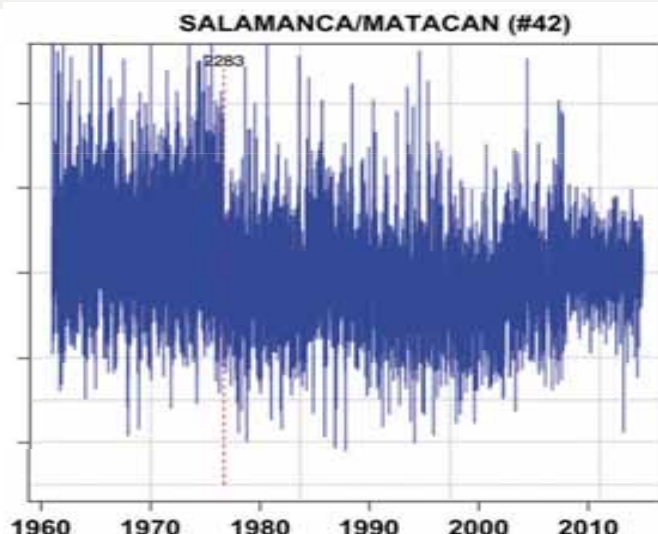
Observed trends in maximum wind

Trends of daily peak wind gusts in Spain and Portugal, 1961–2014

Cesar Azorin-Molina [✉](#), Jose-A. Guijarro, Tim R. McVicar, Sergio M. Vicente-Serrano,
Deliang Chen, Sonia Jerez, Fátima Espírito-Santo

First published: 5 February 2016 [Full publication history](#)

DOI: 10.1002/2015JD024485 [View/save citation](#)



Trends in the 90th percentile of DPWG,

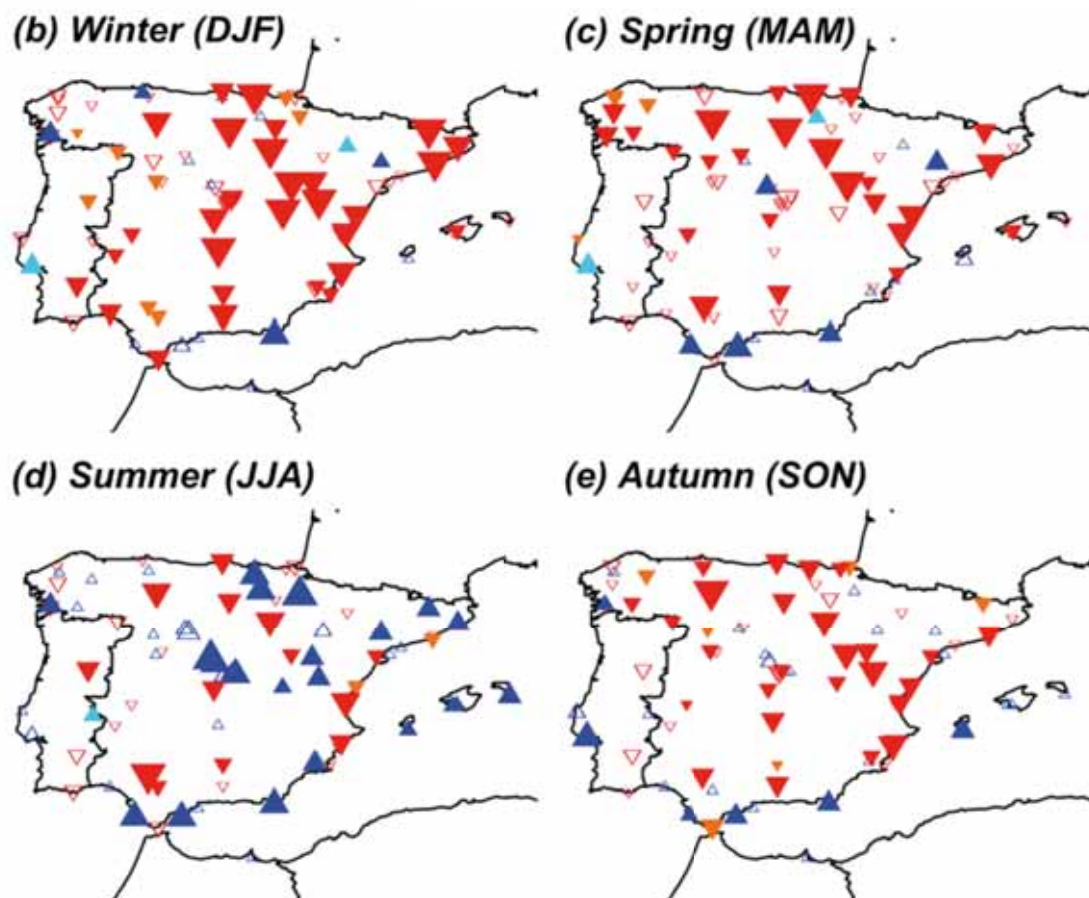
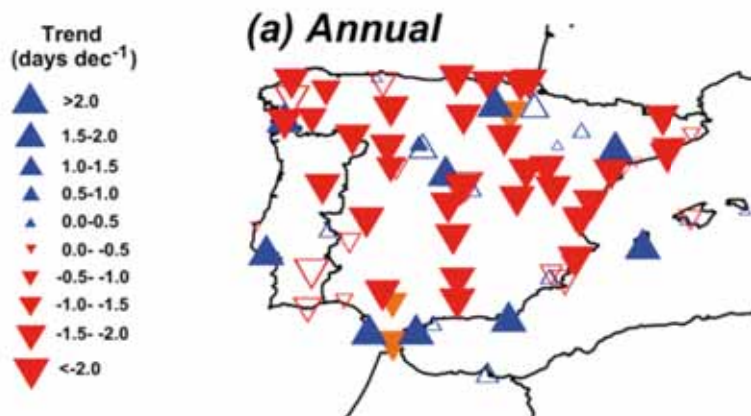


Figure 7. Spatial distribution of the sign, magnitude of trend (d decade^{-1}), and significance (blue and red filled triangles are significant at $p < 0.05$; light blue and orange filled triangles are significant at $p < 0.10$; and nonfilled triangles are not significant at $p < 0.10$) of annual and seasonal number of days exceeding the 54 year 90th DPWG percentile trends for 80 stations for 1961–2014.



Impact of extreme weather
on critical infrastructure



Table 2.2 Indicators based on wind, snow and humidity

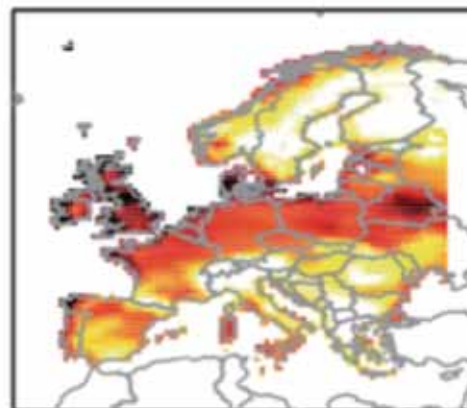
| Wind | Description | Units |
|----------|--|-------|
| FG | Average of daily mean wind speed | m/s |
| FGx1day | Yearly maximum of daily mean wind speed | m/s |
| FGXx1day | Yearly maximum of daily maximum wind speed of gusts | m/s |
| FG05 | Number of days with wind speed > 5 m/s | days |
| FG10 | Number of days with wind speed > 10 m/s | days |
| FG15 | Number of days with wind speed > 15 m/s | days |
| FG25 | Number of days with wind speed > 25 m/s | days |
| FGNN | Number of days with wind speed > NN m/s | days |
| Snow | Description | Units |
| SD1 | Number of days with snow cover | days |
| SD010 | Number of days with snow depth 0-10 mm | days |
| SD1020 | Number of days with snow depth 10-20 mm | days |
| SDx1day | Yearly maximum snowfall | mm |
| SDratio | seasonal snowfall/ average total annual | 1 |
| Combined | Description | Units |
| HU90 | Number of days when the relative humidity (daily mean) is above 90% and mean temperature > 10 °C | days |



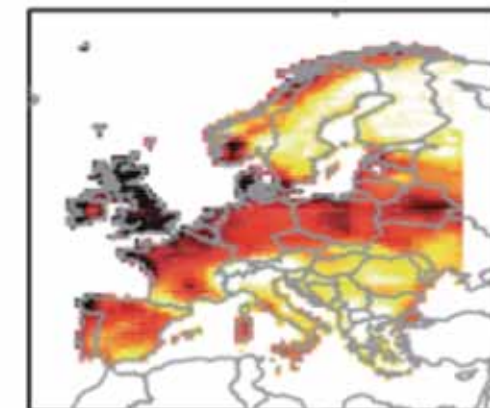
Projected trends in maximum wind

Figure 4.1 Climatology of wind and snow indices for WFDEI data computed on yearly basis averaged over the time period 1981-2000

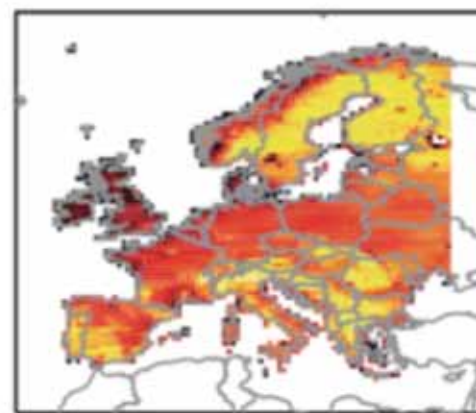
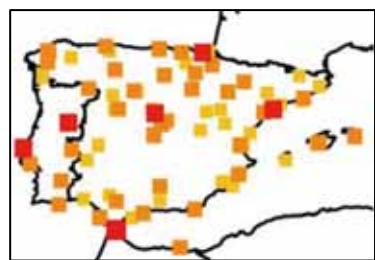
fgx1day: 8.42



fgxx1day: 11.3



fgx1day: 9.75, 0.7



fgxx1day: 24.11, 0.5

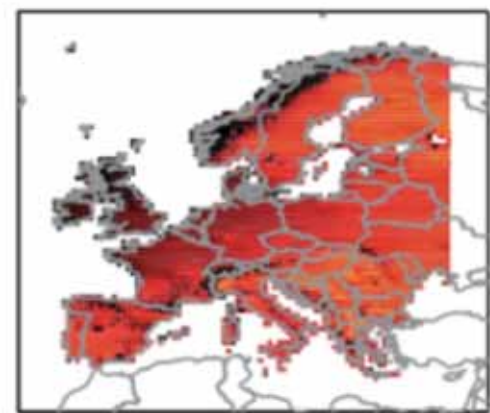
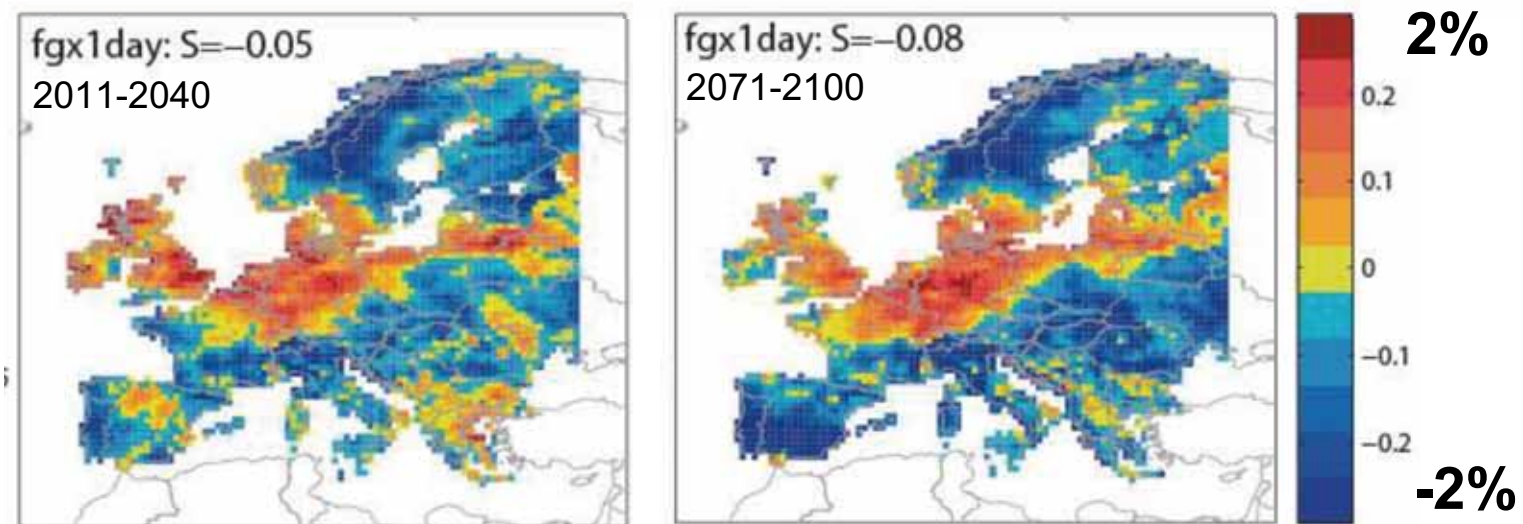
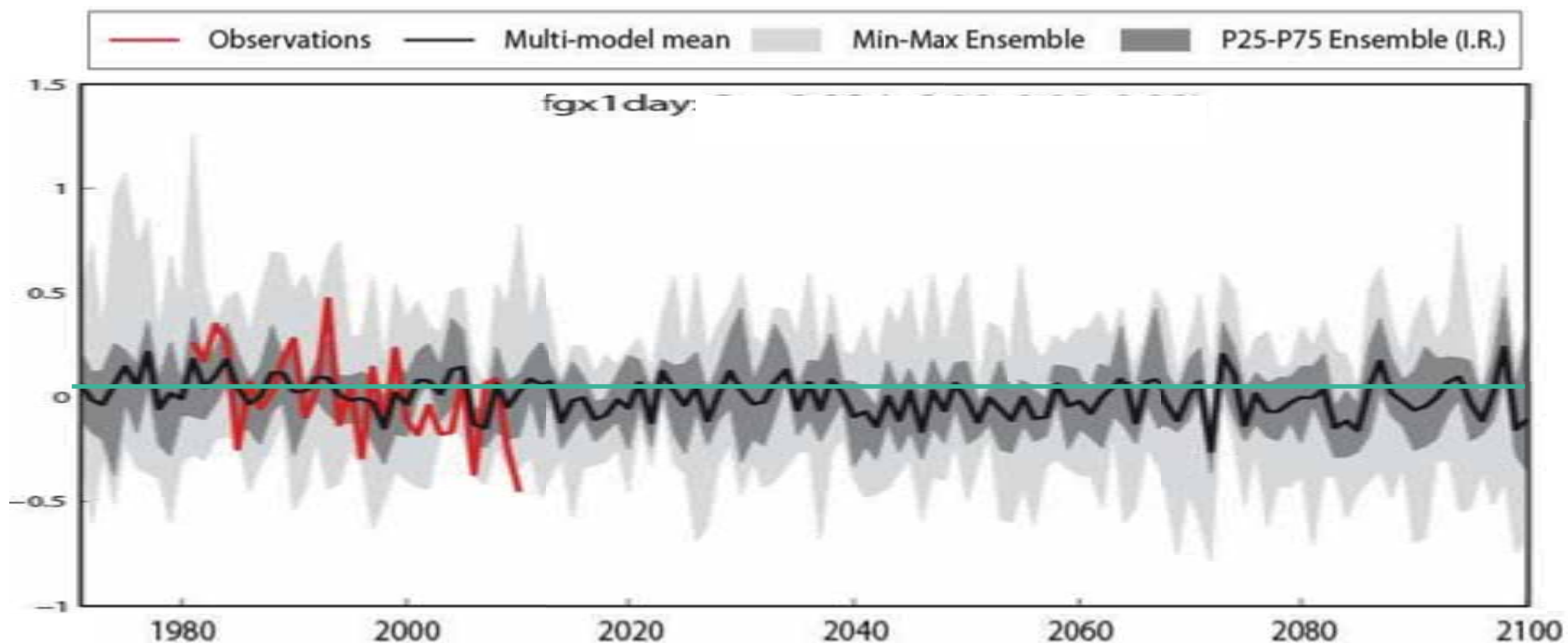


Figure 4.3 Climatology of wind and snow indices for ENSEMBLES data (multimodel mean), computed on yearly basis considering the time period 1981-2000

Projected trends in maximum wind



Future changes in European winter storm losses and extreme wind speeds inferred from GCM and RCM multi-model simulations

M. G. Donat^{1,2}, G. C. Leckebusch¹, S. Wild¹, and U. Ulbrich¹

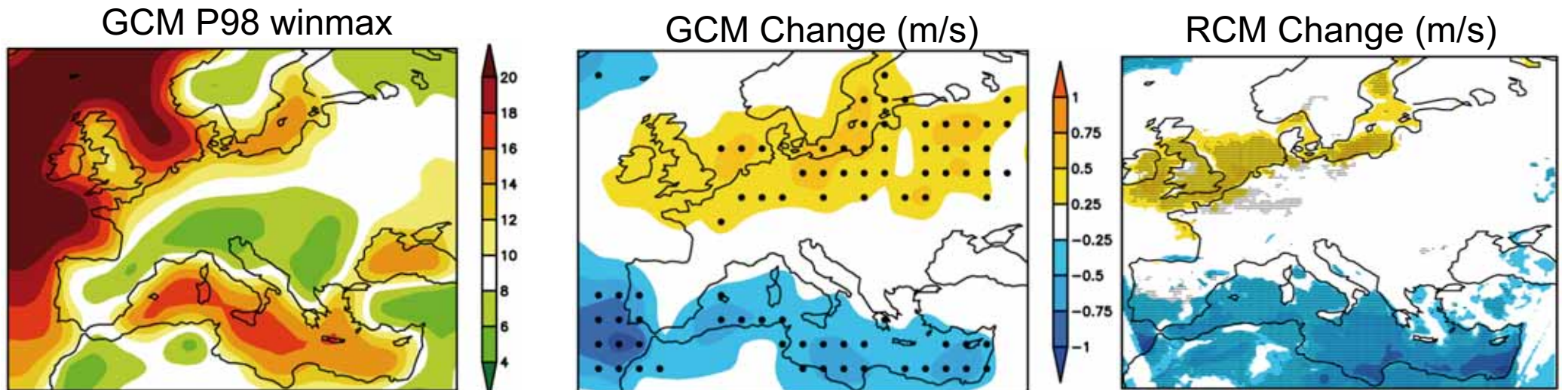
Nat. Hazards Earth Syst. Sci., 11, 1351–1370, 2011

www.nat-hazards-earth-syst-sci.net/11/1351/2011/

doi:10.5194/nhess-11-1351-2011

© Author(s) 2011. CC Attribution 3.0 License.

Results using ENSEMBLES data.



LETTER • OPEN ACCESS

Climate change impacts on the power generation potential of a European mid-century wind farms scenario

To cite this article: Isabelle Tobin *et al* 2016 *Environ. Res. Lett.* 11 034013

EURO-CORDEX

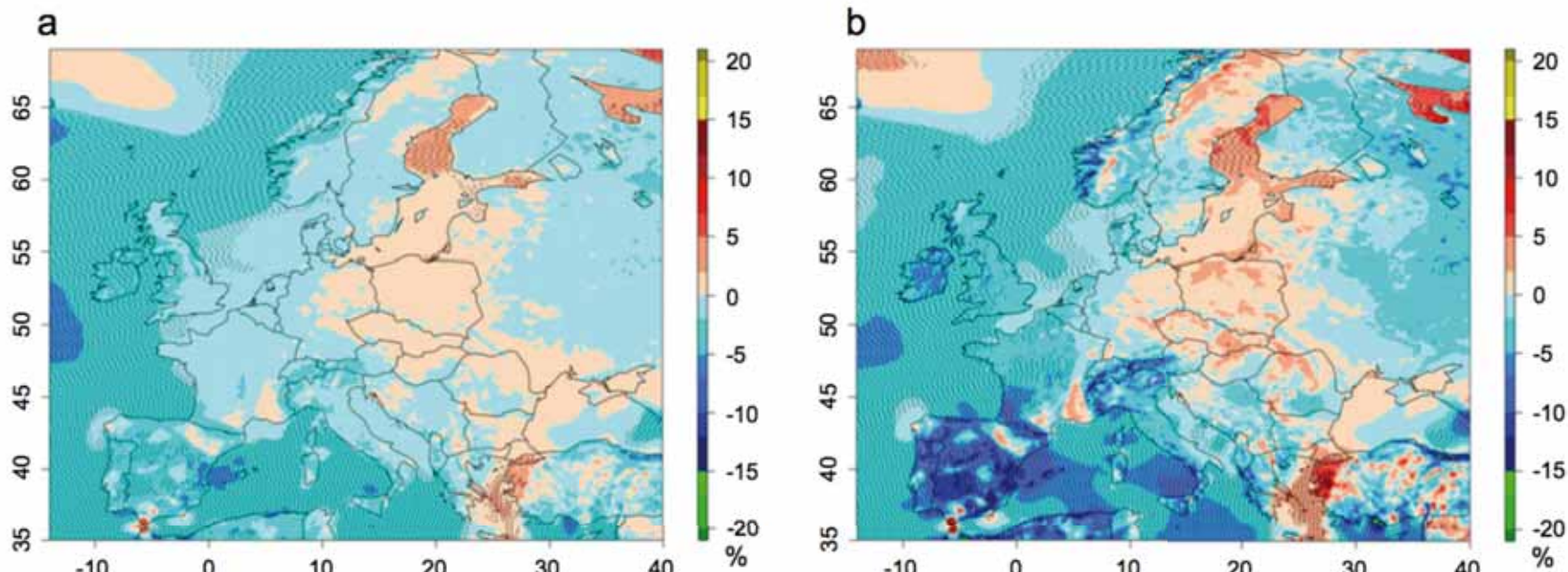


Figure 2. Ensemble mean future changes in wind speed at 10 m (a) and wind power generation potential (b) at the end of the century (2071–2100) relative to the recent 1971–2000 period under scenario RCP8.5. The black dots indicates where the changes are robust (95% significance over the model ensemble, according to Wilcoxon–Mann–Whitney test, and sign agreement over 80% of the models).



The 21st century decline in damaging European windstorms

Laura C. Dawkins¹, David B. Stephenson¹, Julia F. Lockwood², and Paul E. Maisey²

Nat. Hazards Earth Syst. Sci., 16, 1999–2007, 2016
www.nat-hazards-earth-syst-sci.net/16/1999/2016/
doi:10.5194/nhess-16-1999-2016

Klawa and Ulbrich (2003) developed an SSI for the estimation of windstorm losses in Germany. For windstorm event i , this SSI, here denoted L_{98} , was defined as

$$L_{98i} = \sum_{j=1}^J d(s_j) \left(\frac{v_i(s_j)}{v_{98}(s_j)} - 1 \right)^3$$

for $v_i(s_j) > v_{98}(s_j)$,

Roberts et al. (2014)

$$A_{20i} = \sum_{j=1}^J H(v_i(s_j) - 20),$$

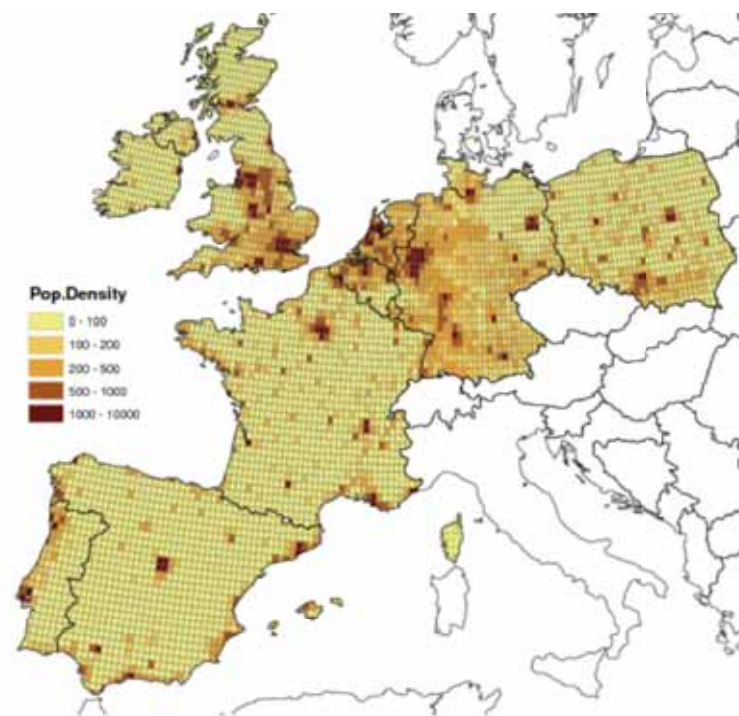
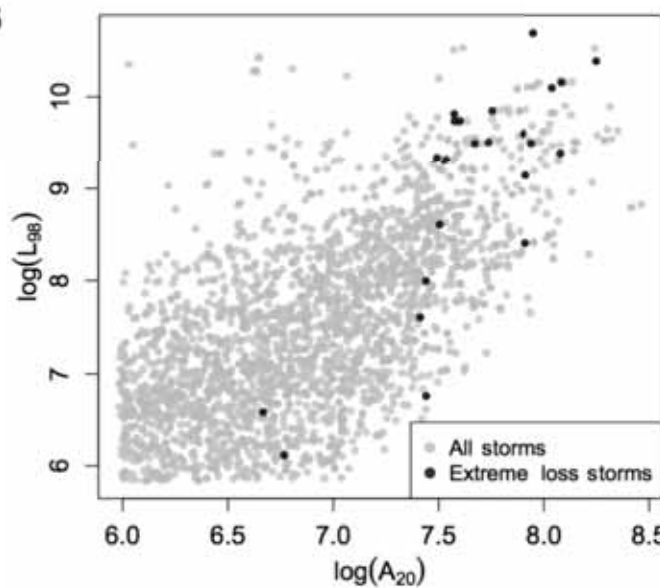


Fig. 1. Population density on a $0.25^\circ \times 0.25^\circ$ grid (source: CIESI)



The 21st century decline in damaging European windstorms

Laura C. Dawkins¹, David B. Stephenson¹, Julia F. Lockwood², and Paul E. Maisey²

Nat. Hazards Earth Syst. Sci., 16, 1999–2007, 2016

www.nat-hazards-earth-syst-sci.net/16/1999/2016/

doi:10.5194/nhess-16-1999-2016

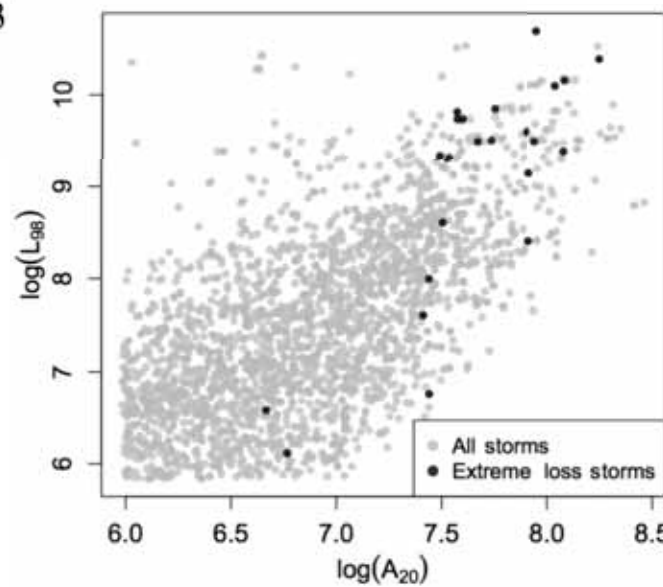
Klawa and Ulbrich (2003) developed an SSI for the estimation of windstorm losses in Germany. For windstorm event i , this SSI, here denoted L_{98} , was defined as

$$L_{98i} = \sum_{j=1}^J d(s_j) \left(\frac{v_i(s_j)}{v_{98}(s_j)} - 1 \right)^3$$

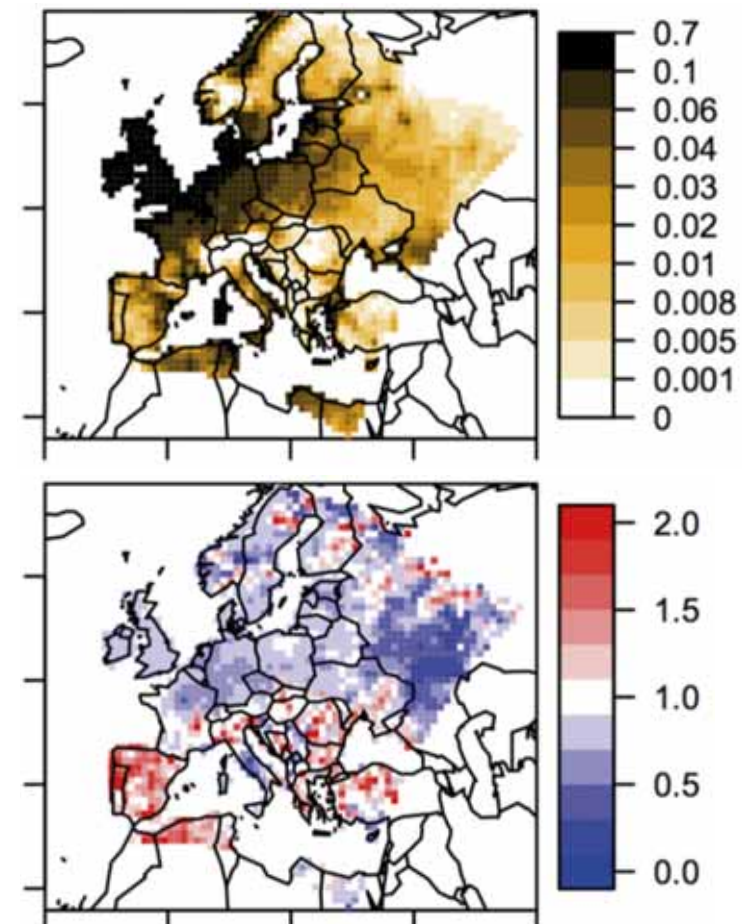
for $v_i(s_j) > v_{98}(s_j)$,

Roberts et al. (2014)

$$A_{20i} = \sum_{j=1}^J H(v_i(s_j) - 20),$$



Relative freq. of exceeding 20 m/s in the 20th century and ratio of the relative frequencies in the 21st and 20th centuries.



Met Office unified model

A diferencia de otras variables (temperatura o precipitación), las proyecciones de cambio climático de viento tienen poca señal a escala global.

A escala regional (Iberia), no se han estudiado suficientemente las proyecciones de viento extremo, así como el potencial de daño derivados, a través de índices y cambios en los patrones físicos..



Proyecciones Regionales de Cambio Climático Para Vientos Extremos en España Para el Siglo XXI

Julio 2017 - Junio 2018



Tracks of the
200 most intense
winter cyclone
tracks
(1989-2009) in
the north Atlantic
(white lines).

